

**Porous Silicon as an Analytical Tool: Investigating the Thin-
film Characteristics of Porous Silicon**

by

Thomas A. Blake

Departmental Honors Thesis

The University of Tennessee at Chattanooga

Department of Chemistry

Project Director: Wendy C. Cory

Examination Date: 30 March 2001

Examining Committee Signatures:

Chairperson, University Departmental Honors Committee

Abstract

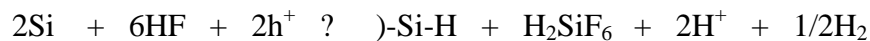
Investigations of the effects of varying reaction conditions for the production of porous silicon layers on doped silicon wafers were performed. Reaction conditions were observed to affect wafers of similar resistivities in a like manner regardless of the wafers being boron-doped (p-type) or phosphorus-doped (n-type). These studies form the basis of a chemical sensor design project and give the conditions for producing porous silicon layers for signal production based on thin-film interference.

Introduction

First observed in the 1950's by Uhlir at Bell Laboratories¹ and then further researched by Turner², porous silicon layers were formed on the surfaces of crystalline silicon wafers during attempts at removing the top layers of the wafers in a process called electropolishing or reverse plating. Electropolishing is a technique utilized by engineers, chemists, and manufacturers to eliminate structural surface flaws and stress lines in a piece of metal by removing the top layer of the material by running an electric current through an acidic solution in which the material rests³. Today the method of producing porous silicon has not changed much from the first attempts; porous silicon lattices are regularly formed by passing electrical current through a hydrofluoric acid (HF) and ethanol solution which is in contact with the surface of a semi-conducting silicon wafer of either n-type or p-type doping. This electrochemical etching reaction leaves behind a vertical network of pores on the nanometer and micrometer scale with depths up to several micrometers⁴⁻⁷.

Throughout the course of the etching reaction, fluorine ions surround and remove silicon atoms that lie along the current pathways that pass through the doped crystal lattice⁸.

Figure 1 – Etching reaction involving HF and doped silicon wafer



The reaction is dependent upon the presence of electron holes (h^+) and will proceed until the current is turned off. However, the regular porous structure is highly dependent upon the length of the reaction, the concentration of acid in the etching solution, and the current density used. An example of this porous structure can be seen in the scanning electron micrograph (Figure 1) taken of one of the wafers etched in this study.

Figure 2 – SEM of porous silicon layer taken by Dr. Steve Symes at NASA in Houston, TX

These pathways through which current can follow in a silicon wafer are present due to impurity doping of the naturally poorly conducting silicon crystal lattice. Doping involves the implantation of atoms other than silicon into the crystal. Such doping can be of two types: n-type involving the addition of an atom with one more electron than silicon (creating a negative hole) or p-type due to the addition of an atom with one less electron than silicon (creating a positive hole). Similar to

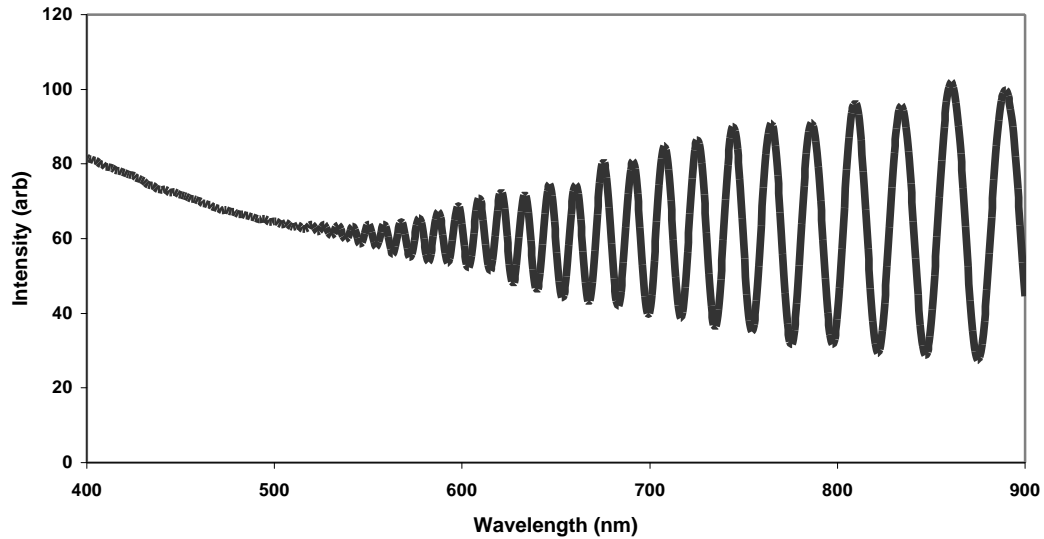
carbon, a silicon atom has four bonding sites with four total valence electrons which it can share with silicon atoms adjacent to it in the crystal lattice. By adding atoms with three valence electrons such as boron or gallium into the lattice, a positive electron hole is produced. This hole promotes electron movement throughout the lattice as the position of the electron hole shifts when an electrical current is applied. Similarly, the addition of atoms such as phosphorus or arsenic, which have five valence electrons, will produce what can be referred to as a negative electron hole. Since the extra electron of the phosphorus does not fit into the four two-electron bonding sites of the silicon atoms, this extra electron will move throughout the crystal lattice in search of a stable resting place. These two forms of introducing electron movement into a silicon lattice increase the ability of the solid to conduct electricity. By adding more dopant atoms, which decreases the resistivity of the wafer, the resistance to current flow of the wafer is reduced drastically; lower doping levels lead to higher resistance and resistivity and lower conductance^{9,10}. This electronic nature of doped silicon wafers allows for chemical reactions promoted by electrical current to occur at the surface of the crystal.

Despite its early discovery, porous silicon only recently became a material of practical interest for chemists when in 1990 Canham first reported the efficient room temperature fluorescence of porous silicon¹¹. In 1992, Doan and Sailor first discussed the optical interference properties of porous silicon layers due to a thin-film effect which was observed during studies investigating the photopatterning of porous silicon surfaces during the electrochemical etching reaction⁸. These developments in the

already well-established field of porous silicon characterization have sparked the interests of researchers pursuing new chemical sensing and optical computing technologies.

The thin-film effect is commonly observed as the bands of color observed on soap bubbles and also oil on wet pavement. In such examples, two different light reflecting surfaces exist in close proximity to each other making a thin film. When incident light strikes such a film, some of the light is reflected from each of the two surfaces. Since the light is reflected differently by the two different surfaces, the wavelengths of the reflected light can constructively and destructively interfere with each other which can be observed as a distinct pattern of light and dark bands known as Newton's rings. These interference fringes can also be observed in the reflectance spectra recorded using a spectrometer. Such is the case also with porous silicon. Light can reflect both off the top and also the bottom of the porous layer, allowing for the reflected light to interfere and produce interference fringes⁹.

Figure 3 – Typical UV-Vis Reflectance Spectrum for Porous Silicon



The amount of fringes over a given wavelength range of light can be directly linked through use of the Fabry-Perot equation (Equation 1) to the distance between the reflecting surfaces.

$$m\lambda = 2\eta L \quad (1)$$

where m is an integer, λ the wavelength of the interference maximum, η is the refractive index of the material, and L is the thickness of the thin-film. Through use of a modified form of Equation 1, an estimated value for the thickness of the porous layer on the surface of an etched silicon wafer can be calculated. The modified equation (Equation 2) is shown below:

$$\eta L = N/(2\Delta\nu) \quad (2)$$

where N is equal to the number of fringe maxima over the inverse of a given wavelength range ($\Delta\nu$) and ηL is the effective thickness of the porous layer. This effect has been used as the basis for chemical sensing utilizing the change in position

of interference wavelength maxima due to changing the thickness of the thin film.

Much of the current research into porous silicon focuses on modifying the silicon surface in order to change the light emitting properties for use in new computing and chemical sensing devices. These surface modifications typically involve the addition of organic molecules which change the fluorescence of the etched wafers^{13,14}. However, there is great potential, as first reported by Jahnshoff and Sailor, to use the specific interference pattern of illuminated porous silicon as the basis for a signal in an interferometric chemical sensor. In the article by Jahnshoff and Sailor, the surface of a porous silicon wafer was modified by the linkage of the biological molecule biotin which will specifically bind the protein streptavidin¹⁵. Since adding bulky molecules to the surface of the porous layer increases the effective thickness (ηL) of the thin-film, the observed interference pattern should shift in relative position in the recorded spectrum. Molecules specific for binding the target analyte were attached to the surface of a porous silicon wafer so that upon addition of an analyte solution, the recognition molecule could bind to the analyte and change the effective optical thickness of the porous layer. This change in effective thickness was evidenced by a red-shift to longer wavelengths in the interference wavelength maxima positions in the reflectance spectra.

The broader scope of the project described in this thesis is to produce such a chemical sensor specific for heavy metals such as mercury in environmental water samples. Mercury ions are relatively small as compared to the much larger streptavidin molecules; the challenge will be whether such a small ion can change the

effective thickness enough to produce a readable shift in the position of the interference wavelength maxima. To undertake a project of such a wide scope, fundamental studies in modifying the porosity and thickness of porous silicon layers by varying reaction conditions were performed. By varying current density (current in milliAmperes over the area of the wafer in cm^2), time of reaction, and the presence of a light source for silicon wafers of both n-type and p-type wafers of different doping levels, the groundwork for a chemical sensor design was laid.

During the electrochemical etch two properties are physically changing: the refractive index (η) which is directly related to the number and size of pores present on the silicon surface, and the thickness (L) of the porous layer, the product of which is the effective optical thickness, (ηL). A set of porous layer effective thickness data as a function of specific reaction conditions was formed for future use in proposed surface modification studies and eventual sensor development.

Experimental

In order to promote the flow of current necessary for the chemical reaction to proceed, it was first necessary to make the semiconducting wafers better conductors. Initial attempts were performed by coating the backs of silicon wafers with a store bought conducting silver epoxy. Although the epoxy was a conductor, the coatings were not very uniform in thickness and did not improve the overall conductivity of the wafers very much as was observed through failed etching attempts.

A chemical precipitation method was then attempted. Known as the Tollen's test once used in organic chemistry classes to determine the presence of product

aldehydes and also in amateur astronomy as a good way to make telescope mirrors¹⁶, the method utilizes a silver nitrate, ammonia, and sodium hydroxide solution from which the complexed silver precipitates out of solution when reduced by aqueous glucose. This chemical method produced thin layers of metallic silver on the backs of silicon wafers. The layers were visually uniform and greatly improved the conductivity of the etching system. In order for the maximum amount of silver to adhere to the silicon surface, the backs of the wafers were rigorously cleaned with soap and distilled water, hydrochloric acid, and finally hexane in order to remove both organic and ionic residues on the surfaces. The wafers were then placed in a large dish filled with a glucose solution. To this was then added a saturated solution containing the necessary reagents. Upon addition, precipitation of the silver was almost immediate and could be seen as a gray/black precipitate which clouded the entire solution. After the formed precipitates had visually settled, the excess solution was decanted and the wafers washed with distilled water. These were then dried in an oven. Conductivity of the silver surfaces was checked using a handheld multimeter.

Once the back of a silicon wafer had been silvered in this manner, the etchable side of the wafer was then cleaned with a dilute hydrochloric acid solution to remove any residual silver that might have coated the top of the wafer during the silvering process. The wafer was then cleaned using several hexane washes to remove any fingerprints and other organic contamination which might have been on the surface. Hexane readily evaporates due to its low vapor pressure, and drying the surface of the wafer to be etched was not necessary.

The actual reaction setup required the use of a Teflon cell made specifically for this purpose (Figure 4). The cell consisted of a solid bottom piece on top of which the wafer would rest. A second Teflon piece with an open well in its center for holding the etching solution was then clamped down on top of the wafer and sealed using a rubber o-ring and screws. To give an electrical lead, a piece of copper foil was placed between the back of the wafer and the solid Teflon piece. The total amount of the wafer which would be exposed to the HF solution was 1.5cm^2 . The etching solution consisting of 1mL of absolute ethanol and 1mL of 49% aqueous hydrofluoric acid was then added to the well in the top of the etching cell. The electrical circuit was completed by connecting the constant power source with alligator clamps to the copper flag under the bottom of the wafer and a platinum wire electrode which rested in the acid solution but not touching the actual silicon wafer. Current was run in the direction from the platinum electrode through the silicon wafer and out the copper flag and was monitored by having a voltammeter in series with the circuit. After an etch was completed, the acidic solution was removed and disposed of and the surface of the wafer washed with excess ethanol. The wafer was then dried under a stream of nitrogen and removed from the Teflon cell.

Figure 4 – Experimental Setup for Electrochemical Etching Reaction

The effects of different reaction times and current densities were studied by keeping one of the variables constant while changing the other. Studies of the effects of a light source on the production of the thin-film layers were also performed using a dark box and a focused 60W or 75W incandescent white light. This was of interest since p-type wafers are usually etched in the dark while n-type wafers require a light source. This is because the etching reaction depends on the traveling of positive electron holes to the platinum cathode. These holes are readily available in p-type wafers, but they must be created in n-type wafers. An energy source such as white light allows the creation of such holes by exciting electrons from the valence shell to a higher energy level, leaving behind an electron hole.

Scanning electron microscopy (SEM), which produces images of surfaces with sub-micrometer resolution, was performed on two of the etched silicon wafers. From the SEM micrographs, the typical and expected vertical network of pores was observed and verified. For the chips studied, etch depth is less than 50 μ m. These wafers were imaged at NASA (Figure 2). Unfortunately, limited access to an SEM made further imaging studies prohibitive. For this reason, actual porosity values were not obtained, although a poorly resolved SEM imaged at DuPont gave an estimated pore diameter of approximately 50nm. However, the effective thickness (ηL) measurements reported here do not depend on SEM data.

Diffuse reflectance Fourier Transform infrared spectroscopy (DRFT-IR),

which gives information about the molecular composition of a solid surface, was performed on many of the first wafers etched. The technique utilizes the vibration of bonds between atoms in the compounds being studied. These vibrations fall in the same order of magnitude as infrared radiation in wavenumbers (cm^{-1}). Characteristic unsymmetrical vibrations are excited when the molecule absorbs infrared radiation. To perform this technique upon a reflective silicon crystal, an unetched silicon wafer was used for a background reading, and infrared radiation was simply reflected off the surfaces of the sample wafers. The completion of the etching reaction was confirmed by this method as evidenced by a characteristic Si-H stretch at approximately 2100cm^{-1} . Interestingly, interference fringes were observed in many of these spectra due to the thin-film characteristics of the material. This did make the analysis of the spectra more complicated, but the necessary data was still obtainable.

Two different methods of performing reflectance UV-visible spectroscopy were pursued to observe the interference effect and to measure the effective thickness of each wafer. For both methods, an unetched silicon wafer was used as the background reading since unetched silicon wafers do not act as a thin-film producing no interference fringes in their reflectance spectra. The first involved the use of a version of the chemical sensor field method setup using an Ocean Optics portable spectrometer, a colored light emitting diode (LED) as the light source, fiber optics, and a laptop computer for signal analysis.

The second setup used a Spectral Instruments CCD Array UV-Vis Spectrophotometer, using the supplied tungsten white light source of 400-900nm in

wavelength, and a fiber optic reflectance probe which could rest directly perpendicular to the wafer in contact with the surface. This setup was found to be better for our fundamental studies as it gave a bigger range of wavelengths over which to observe interference allowing for more accurate calculations of effective thickness (ηL). By counting the number of maxima in the interference spectra produced by this method, the effective thickness (ηL) could be calculated using the modified Fabry-Perot equation $\eta L = N/(2\Delta\nu)$. The information gained by using this technique was used to directly correlate the changing reaction conditions with the thickness of the porous layers produced.

Data

The following tables present the variable changed in each reaction set as well as observations made from the resultant reflectance spectra including the wavelength range ($\Delta\lambda$) in nanometers over which interference fringes were observed (used to determine $\Delta\nu$ as $\Delta\nu = 1/\lambda$), the number of fringes (N) in that region, and the calculated thickness (ηL) of the porous layers in micrometers. Four different sets of wafers were studied, each varying in dopant type and amounts.

N-type 0.09 W cm

Table 1 shows the effective thicknesses obtained using a platinum ring electrode while changing the current density at a constant reaction time of 30s. The reactions were performed in the dark.

Table 1

Wafer	mA/cm^2	$\Delta\lambda$	N	hL (mm)
S20	133	400	20	4.0
S21	200	380	25	4.8
S22	267	385	26	5.0
S15	320	350	24	4.2
S26	333	370	27	5.0
S27	400	380	26	4.9
S16	433	380	31	5.9
S30	467	360	24	4.3
S31	533	340	17	2.9

Table 2 gives the effective thickness values for wafers etched in the dark with varying current density for a reaction time of 30s. However, for this set a platinum mesh electrode was used in the reactions.

Table 2

Wafer	mA/cm^2	$\Delta\lambda$	N	hL (mm)
S36	67	420	16	3.4
S37	133	370	17	3.1
S38	200	450	18	4.1
S40	333	360	21	3.8
S42	333	400	24	4.8
S43	333	325	19	3.1

At this point, it was decided that the mesh electrode produced the most uniform current distribution. The mesh electrode was used for all future studies. Also these studies clearly show that it is not necessary to use a light source to make porous silicon on n-type wafers.

N-type 0.5-1.0 W cm

Table 3 lists effective thicknesses obtained while changing etch time at a constant current density of 50mA/cm^2 . These reactions were performed under focused light from a 60W tungsten light bulb.

Table 3

Wafer	Time (s)	$\Delta\lambda$	N	hL (mm)
N41	15	530	0	0
N40	30	530	0	0
N39	45	530	0	0
N38	60	530	0	0
N37	90	530	1	0.27
N36	120	530	2	0.53
N42	180	530	1	0.27
N43	240	530	1	0.27
N44	300	530	1	0.27
N45	420	530	0	0

The effective thickness was found to increase with time up to 120s and then drop off in measured thickness as evidenced by less interference fringes. As the effective thickness decreased, porous silicon layers that fluoresced under ultra-violet light began to be formed.

In Table 4, etching reactions were performed at a constant current density of $10\text{mA}/\text{cm}^2$ while changing time of the etch. This set of reactions was performed under the focused light of a 75W tungsten light bulb.

Table 4

Wafer	Time (s)	$\Delta\lambda$	N	hL (mm)
N31	15	530	1	0.27
N30	30	530	2	0.53
N32	45	530	2	0.53
N33	60	530	3	0.80
N34	90	530	3	0.80

N35	120	530	1	0.27
-----	------------	-----	---	-------------

Again, effective thickness was found to increase with time to a point and then decrease, and fluorescent layers were formed in some of the longer etched wafers.

The wafers in Table 5 were etched at a constant current density of 0.67mA/cm^2 while changing etch time under the light of a focused 60W light bulb.

Table 5

Wafer	Time (s)	$\Delta\lambda$	N	hL (mm)
N47	15	530	0	0
N46	30	530	0	0
N48	45	530	0	0
N49	60	530	0	0
N50	90	530	0	0
N51	120	530	1	0.27
N52	180	530	1	0.27
N53	300	530	1	0.27
N54	420	530	2	0.53
N55	600	530	3	0.80
N70	660	530	3	0.80
N68	780	530	2	0.53
N69	900	530	2	0.53
N56	1200	530	2	0.53

The same trend is observed. It is important to note that no real difference in the porous silicon formed using a 60W or 75W bulb was observed.

P-type 0.005-0.018 W cm

Table 6 contains the effective thickness values of wafers etched for 30s in the dark under varying current densities.

Table 6

Wafer	mA/cm²	$\Delta\lambda$	N	hL (mm)
P10	0.67	530	2	0.53
P9	6.7	530	5	1.3
P8	17	505	6	1.5
P7	33	480	9	2.2
P6	67	480	14	3.4
P4	200	435	20	4.4
P1	333	490	23	5.6

The effective thickness was found to increase with current density. After 333mA/cm², the porous layers were observed to flake off of the surface. Once this destruction of the attached porous layers had occurred, effective thickness measurements could not be made, and the wafers were neither usable nor included in the data tables.

Table 7 gives the effective thickness values observed while changing the current density of the etching reactions at a constant time of 30s. The reactions were performed under focused light from a 60W tungsten light bulb.

Table 7

Wafer	mA/cm²	$\Delta\lambda$	N	hL (mm)
P29	0.67	530	2	0.53
P28	6.7	530	5	1.3
P27	17	505	6	1.5
P26	33	480	14	3.4
P25	67	485	18	4.4
P23	200	480	23	5.5
P21	267	440	22	4.8

It is clear that the presence or absence of a light source did not affect the production of porous silicon, which increased in effective thickness with current density to a point and then began flaking off from the surface.

The wafers in Table 8 were etched with a constant current density of 67 mA/cm^2 while varying the etch time in the dark

Table 8

Wafer	Time (s)	$\Delta\lambda$	N	hL (mm)
P12	4.8	530	4	1.1
P11	15	515	9	2.3
P13	45	480	18	4.3
P14	60	480	18	4.3
P15	90	470	24	5.6
P16	120	400	37	7.4
P17	180	340	34	5.8
P18	240	340	41	7.0
P19	300	340	44	7.5

The effective thickness increased with time until flaking of the surface was observed.

Table 9 shows the effective thickness values obtained for wafers etched at a constant current density of 333 mA/cm^2 while varying time. These wafers were etched in the dark.

Table 9

Wafer	Time (s)	$\Delta\lambda$	N	hL (mm)
P30	60	350	24	4.2
P31	120	370	42	7.8
P32	180	370	24	4.4
P33	240	530	0	0

The effective thickness increased with time until flaking of the surface occurred as observed for similar trials.

P-type 8-12 W cm

Table 10 gives the values of effective thickness for wafers etched in the dark while varying the time at a constant current density of 10 mA/cm^2 .

Table 10

Wafer	Time (s)	$\Delta\lambda$	N	hL (mm)
S103	30	530	0	0
S102	60	530	2	0.53
S101	90	530	4	1.1
S117	120	530	6	1.6
S104	240	500	8	2.0
S105	360	530	0	0

For this current density, effective thickness was observed to increase with time until 240s, and then drop off which was observed as a lack of interference fringes in the reflectance spectra of wafers etched past 240s.

Table 11 contains effective thickness values calculated for wafers etched in the dark at a constant current density of 33mA/cm² while varying the time of reaction.

Table 11

Wafer	Time (s)	$\Delta\lambda$	N	hL (mm)
S106	30	530	6	1.59
S107	45	530	6	1.59
S108	60	530	6	1.59
S109	90	490	7	1.72
S110	120	440	7	1.54
S111	180	490	10	2.45
S114	210	530	0	0
S112	240	530	0	0
S113	300	530	0	0

For this current density, effective thickness was observed to increase with time until 180s, and then drop to zero.

The wafers in Table 12 were etched at a constant current density of 10mA/cm² for different reaction times under focused light from a 60W light bulb.

Table 12

Wafer	Time (s)	$\Delta\lambda$	N	hL (mm)
S115	60	530	3	0.80
S116	120	530	6	1.59

These two samples were shown to demonstrate that the absence or presence of light had little effect on the production of porous silicon.

Conclusions

From what was observed, it was determined that the sets of data that were collected throughout the course of this project can be separated into the two general categories: *high resistivity wafers* and *low resistivity wafers*. Generalizations about each data set span both n-type and p-type wafers with doping levels in similar ranges.

High Resistivity Wafers

Figures 5, 6, 7, and 8 graphing represent the data in tables 4, 5, 10 and 11.

Figure 5 - Effective thickness vs. time for n-type wafers etched at 0.67mA/cm^2

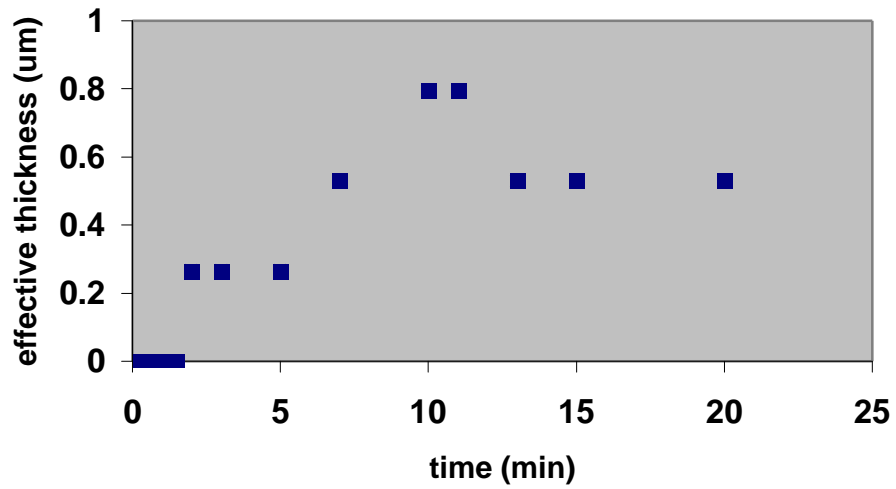


Figure 6 - Effective thickness vs. time for n-type wafers etched at 10mA/cm²

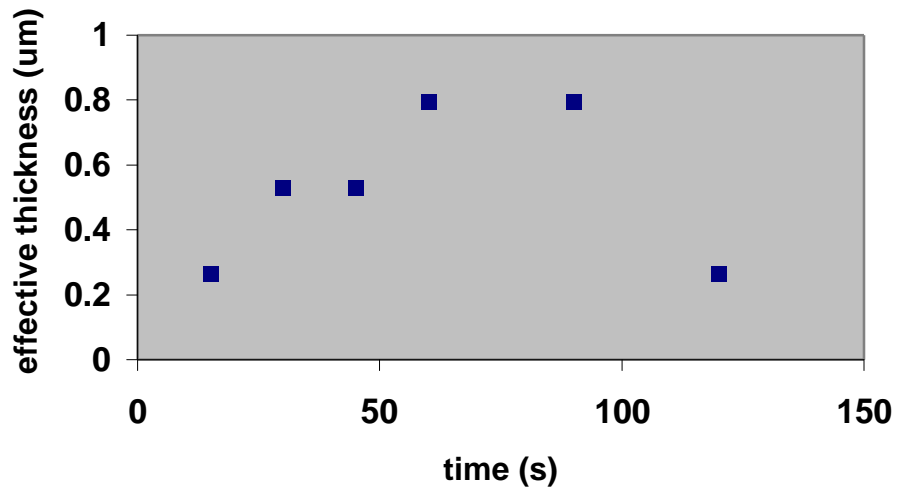


Figure 7 - Effective thickness vs. time for p-type wafers etched at 10mA/cm²

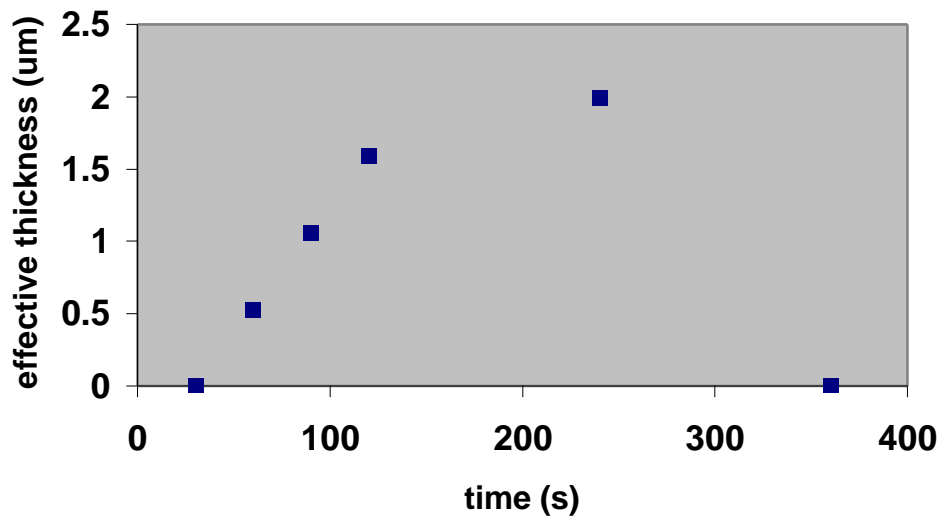
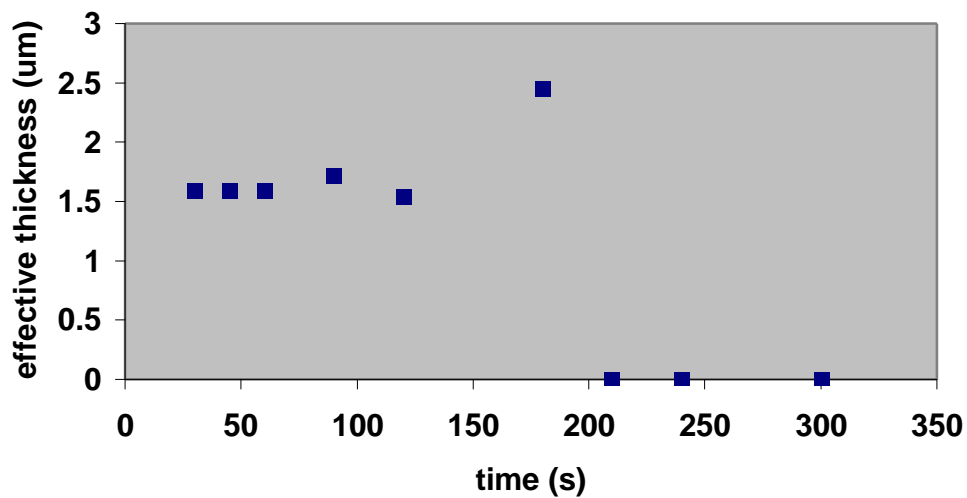


Figure 8 – Effective thickness vs. time for p-type wafers etched at $33\text{mA}/\text{cm}^2$



As shown in the plotted trends (Figures 5-8) for the set of high resistivity silicon wafers (lower doping levels), the thin-film effect was observed for both p-type and n-type doped wafers when etched at lower current densities ranging from $0.67 - 33 \text{ mA}/\text{cm}^2$. From initialization of the etching reaction, effective thickness, as

calculated using Equation 2, increases with time to a maximum and then declines. This observation is attributed to the porous layer increasing in thickness during the etching reaction at the same time that the pores themselves increase in diameter, resulting in a decrease in the refractive index (η). An increase in pore size with time has been reported as the cause of increasing porosity and decreasing η ¹⁷.

We attribute the observed decline in effective thickness and thin-film character to the influence of increasing porosity overcoming that of increasing layer thickness. Once the diameter of the pores is too large, the thin-film effect is not observed due to a lack of two virtually flat surfaces that can reflect light. Both the n-type and p-type wafers exhibit thin-film interference patterns for similar current densities and times, resulting in effective thicknesses of less than 5 micrometers in depth.

Low Resistivity Wafers

Figure 9 graphically represents the data from tables 6 and 7. Figure 10 represents the data from Table 8.

Figure 9 - Effective thickness vs. current density for p-type wafers etched for 30s (triangular data points for wafers etched under light, square points for wafers etched in the dark)

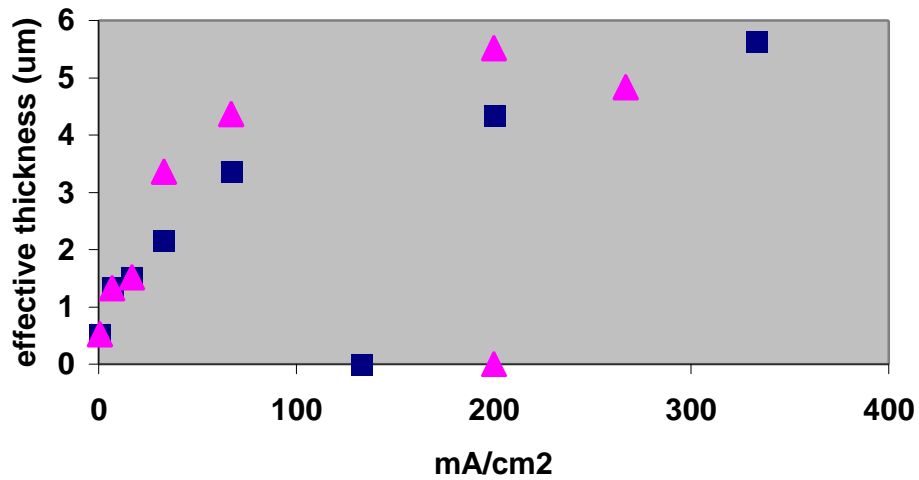
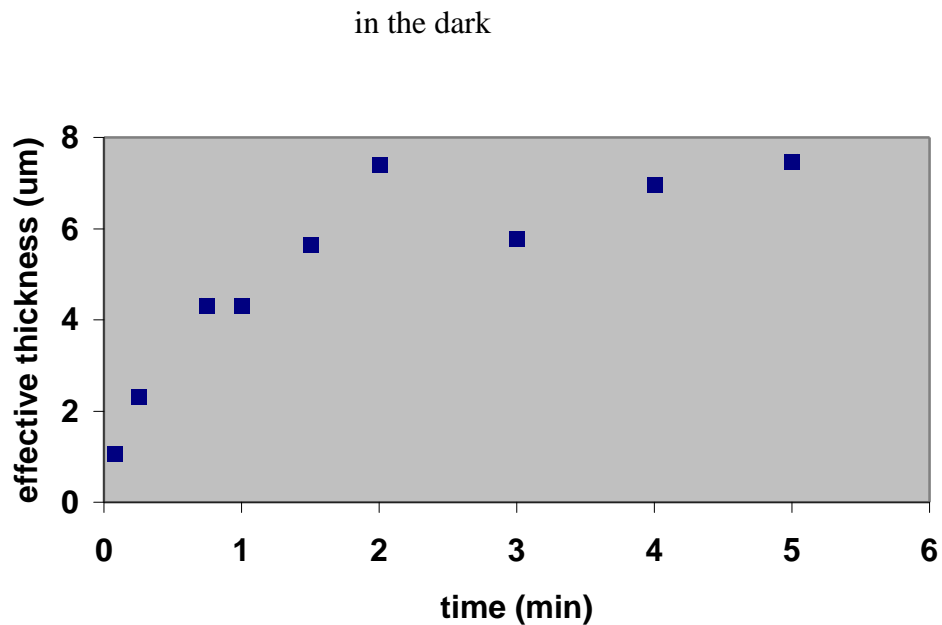


Figure 10 - Effective thickness vs. time for p-type wafers etched at $67\text{mA}/\text{cm}^2$



Thin-film interference was observed, as shown in the plotted trends (Figures 9-10), for p-type and n-type wafers of lower resistivity (higher doping levels) when etched at higher current densities. From initialization of the etching reaction, the effective thickness increases with time to a maximum then drops to zero. We attribute this drastic drop in character to the etching reaction reaching a point where electropolishing, or stripping of the top layer of the wafers, occurs. Evidence of electropolishing included the etched wafers having extremely nonhomogenous surfaces and the etching solutions from those reactions containing visible flakes of the silicon. For some of the trials run, electropolishing did not occur and effective thickness continued increasing with time. N-type and p-type silicon wafers of lower resistivity exhibited thin-film character when etched under similar conditions up to 333mA/cm^2 resulting in calculated effective thicknesses of up to 10 micrometers. One reason that electropolishing is observed only with the lower resistivity wafers in

the conditions used is because of the higher doping levels and higher conductivity of these wafers which allows current to flow more readily through the wafers. In this way, the wafer has more metallic character, and electropolishing occurs more readily in metals. For the higher resistivity wafers, electropolishing was not observed for the conditions used because increasing porosity supercedes the thin-film effect before the extreme electropolishing range of conditions can be met.

Also for this series, a tungsten white light bulb (60W or 75W) was used for some of the trials. The light from this source was focused onto the surface of the wafers for the duration of the etching reaction. For the trials performed, little difference was observed in the produced porous silicon as compared to wafers etched under the same conditions except in a dark box, with some exceptions for the n-type wafers etched at higher current densities. Studies into the dependence on a light source by the etching reaction were not the main focus of the overall study and more in-depth research using more intense light sources should be performed. Interestingly though, despite the highly reported need of a strong light source for the etching reaction on n-type wafers to produce photoluminescent porous silicon layers, n-type wafers etched in the dark do show thin-film character very similar to their p-type counterparts.

As a result of this study, further work into the chemical sensor design portion of the project can continue. Determining a surface modification pathway will be the next step in the process of forming the proposed interferometric sensor for mercury in water samples. Having performed this set of work, future researchers on this project

will know specific conditions to produce desired porous silicon layers which exhibit optimal numbers of interference fringes in their respective reflectance spectra.

Works Cited

- 1) Uhlir, A. *Bell System Technical Journal*, **35**, (1956) 333.
- 2) Turner, D.R. *Journal of the Electrochemical Society*. **105**, (1958) 402-408.
- 3) "Electropolishing: A User's Guide." <http://www.ntaindustries.com/elecplsh.html>.
printed on 27 November 2000
- 4) Cullis, A.G.; Canham, L.T.; and Calcott, P.D.J. *Journal of Applied Physics*. **82**, (1997) 909-965.
- 5) Sailor, M.J.; Heinrich, J.L.; and Lauerhaas, J.M. *Semiconductor Nanoclusters: Studies in Surface Science and Catalysis*. **103**, (1996) 209-233.
- 6) Searson, P.C.; Macauley, J.M.; and Prokes, S.M. *Journal of the Electrochemical Society*. **139**, (1992) 3373-3378.
- 7) Smith, R.L. and Collins, S.D. *Journal of Applied Physics*. **71**, (1992) R1-R22.
- 8) Lehmann, V.; Gosele, U. *Applied Physics Letters* **58**, (1991) 856.
- 9) Tipler, P.A. *Physics for Scientists and Engineers*. 3rd Ed. Worth Pub: New York.
(1991) 1063-1066, 1305-1313.
- 10) Shriver, D.F. and P.W. Atkins. *Inorganic Chemistry*. 3rd Ed. W.H. Freeman:
New York. (1999) 110-112.
- 11) Canham, L.T. *Applied Physics Letters*. **57**, (1990) 1046-1048.
- 12) Doan, V.V. and Sailor, M.J. *Science*. **256**, 26 June 1992.
- 13) Buriak, J.M. *Chemical Communications*. **12**, (1999) 1051-1060
- 14) Lauerhaas, J.M. ; Credo, G.M. ; Heinrich, J.L. ; and M.J. Sailor. *Journal of the American Chemical Society*. **114**, (1992), 1911-1912.
- 15) Janshoff, A. ; *et al.* *Journal of the American Chemical Society*. **120**, (1998) 12108-12116.
- 16) Ingalls, A.G. *Amateur Telescope Making Advanced*. Munn & Co: 1937. 477-482.

17) Bomchil, G.; Herino, R.; Barla, K.; and J.C. Pfister. *Journal of the Electrochemical Society*. **130**, (1983), 1611.

Works Consulted

- Ban, T.; *et al.* *Japanese Journal of Applied Physics*. **33**, (1994) 5603-5607.
- Berger, M.G.; *et al.* *Thin Solid Films*. **255**, (1995) 313-316.
- Bright, V.M.; Kolesar, Jr., E.S.; Sowders, A.M. *Optical Engineering*. **36**, (1997) 1088-1093.
- Curtis, C.L. ; *et al.* *Journal of the Electrochemical Society*. **140**, (1993) 3492-3494.
- Doan, V.V.; Penner, R.M.; and Sailor, M.J. *Journal of Physical Chemistry*. **97**, (1993) 4505-4508.
- Frohnhoff, S. and Berger, M.G. *Advanced Materials*. **6**, (1994) 963-965.
- Herino, R. *et al.* *Journal of the Electrochemical Society*. **184**, (1987) 1994-2000.
- Ingle, Jr., J.D. and Crouch, S.R. *Spectrochemical Analysis*. Prentice Hall, New Jersey. 1988.
- Lazarouk, S.; *et al.* *Thin Solid Films*. **297**, (1997) 97-101.
- Lin, V.S.Y.; *et al.* *Science*. **278**, (1997) 840-843.
- Rossow, U.; *et al.* *Thin Solid Films*. **255**, (1995) 5-8.
- Sze, S.M. *Physics of Semiconductor Devices 2nd Ed.* John Wiley & Sons, New York, 1981.